ResearchGate

See discussions, stats, and author profiles for this publication at: https://www.researchgate.net/publication/6883108

X-ray Diffraction Study into the Effects of Liming on the Structure of Collagen

ARTICLE *in* BIOMACROMOLECULES · SEPTEMBER 2006

Impact Factor: 5.75 · DOI: 10.1021/bm060250t · Source: PubMed

CITATIONS
28

READS
37

3 AUTHORS, INCLUDING:

Tim J Wess
Charles Sturt University
111 PUBLICATIONS **3,098** CITATIONS
SEE PROFILE

Craig Kennedy
Heriot-Watt University
41 PUBLICATIONS **748** CITATIONS
SEE PROFILE

Available from: Craig Kennedy
Retrieved on: 26 January 2016

X-ray Diffraction Study into the Effects of Liming on the Structure of Collagen

Clark A. Maxwell,* Tim J. Wess, and Craig J. Kennedy

Biophysics Division, School of Optometry and Vision Sciences, University of Cardiff, Redwood Building, King Edward VII Avenue, Cathays Park, Cardiff, Wales, United Kingdom CF10 3NB

Received March 17, 2006; Revised Manuscript Received May 26, 2006

The manufacture of parchment from animal skin involves processes that remove hair, fats, and other macromolecules. Although it is well understood that the collagen fibers "open up" during processing, this study uses small and wide-angle X-ray diffraction to measure quantitatively the changes induced at the nanoscopic and microscopic levels. The axial rise per residue distance within the collagen molecules is unaffected by salt and lime treatments. Salting of the hides appears to remove noncollagenous materials. The intermolecular lateral packing distance between the hydrated collagen molecules (1.4 nm) increases after salting (∼1.5 nm) and liming (∼1.55 nm); drying is responsible for a reduction to ∼1.2 nm in all samples. The axial staggered array (*d* spacing) is reduced by 1 nm after liming and is unaffected by drying. The average fibril diameter increases from 103.2 to 114.5 nm following liming, and the fibril-to-fibril distance increases from 122.6 to 136.1 nm.

Introduction

A major byproduct of the meat industry is animal hides, which provides a valuable source of collagen based materials. Collagen products include leather and parchment, and as gelatin, it is used in the food industry, photographic industry,[1] and pharmaceutical industry for capsules to aid oral drug delivery. Collagen is the major extra cellular matrix protein and forms naturally into polymers that associate together into specific hierarchical structures. The formation of these structures and their association with noncollagenous macromolecules such as the proteoglycans chrondroitin sulfate and dermatan sulfate[2−4] is fundamental to the high level of tensile strength and flexibility that collagen gives to tissues, such as tendon, ligaments, and skin.[5]

Hides usually undergo a series of primary treatments such as salting, liming, and mechanical abrasion in order to partially preserve, remove hair (and other noncollagenous macromolecules), and alter the overall mechanical properties of the tissue.[5] Parchment manufacture is a well established use of hide where the steps in manufacture are representative of general hide treatments and finishing processes resulting in a variety of products. For example, the use of tanning agents in the manufacture of leather and not in parchment is the fundamental difference between both manufacturing processes. Liming and salting have remained key steps in parchment production for at least the last millennia and is a relatively modern method compared to that used to make the Dead Sea Scrolls. Examining the molecular alterations engendered in the tissue by salting and liming protocols will therefore give useful information applicable to many different collagen based manufacturing processes.

To date the changes in collagen and associated molecules at the molecular, nanoscopic, and microscopic levels brought about by hide treatments are not well described in the literature. Terms such as "opening up" of the collagen fibers is often used to describe the effects of the processes such as liming and salting without a firm structural basis.[6] The purpose of the data presented here is to describe quantitatively the alterations to collagen structure in the processes of salting, liming, and drying that are used in parchment manufacture but are also representative of many other collagen treatments.

Collagen based tissues such as skin are hierarchically organized materials where there is an intimate relationship and connectivity between the molecular structure relating to the helical organization within individual collagen molecules. The well-defined nanoscopic axial and lateral organization of locally associated collagen molecules and thence the organization of discrete fibrillar structures as shown in Figure 1 produce a functional tissue.

Collagen molecules are composed of three polypeptide chains that form a triple helix. The collagen molecules are staggered axially relative to their neighboring molecules by *d*, ∼67 nm in tendon or ∼65.5 nm in skin. This arrangement is known as the Hodge−Petruska model.[2,7,8]

The *d* repeat is a characteristic feature of collagen. The stagger leaves a gap between linearly adjacent molecules as the molecular length (300 nm) is not an exact multiple of the *d* period, which results in a gap region and an overlap region within each *d* repeat. The gap region comprises 0.54 of *d*, and the overlap subsequently comprises 0.46 of *d*.[9] Of the 29 known collagen types, types I, II, III, V, and XI are capable of forming fibrils. The collagen molecules are orientated forming cylindrical objects with diameters ranging between 10 and 500 nm.

X-ray diffraction was used quantitatively to measure changes at different levels of the collagen structural hierarchy, from intra- and intermolecular interactions to analysis of the size of the collagen fibrils in the hydrated and dehydrated states that comprise fundamental elements of the parchment making process. Due to its minimal sample preparation requirements, X-ray diffraction has great potential when analyzing parchments that should not be damaged, as they can be valuable historical materials. It is therefore an important technique, which can be used to analyze and compare both historical and modern materials.

* Corresponding author. Tel: +44 29 2087 0203. Fax: +44 29 2087 4859. E-mail: MaxwellCA@cardiff.ac.uk.

10.1021/bm060250t CCC: $33.50 © 2006 American Chemical Society
Published on Web 07/22/2006

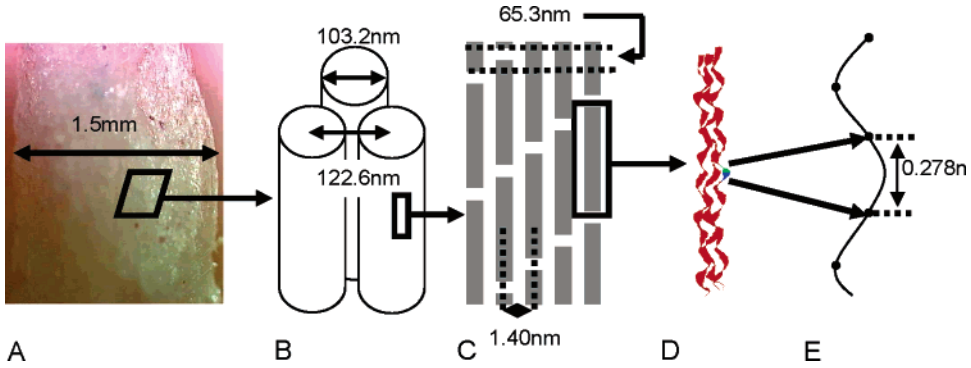

Figure 1. Collagen hierarchy from the microscopic down to the molecular. (A) An image of untreated bovine hide. (B) Fibril packing. (C) Microfibril packing. (D) Collagen triple helix. (E) Helical rise per residue distance. Diagram is for hydrated untreated bovine hide and is not to scale.

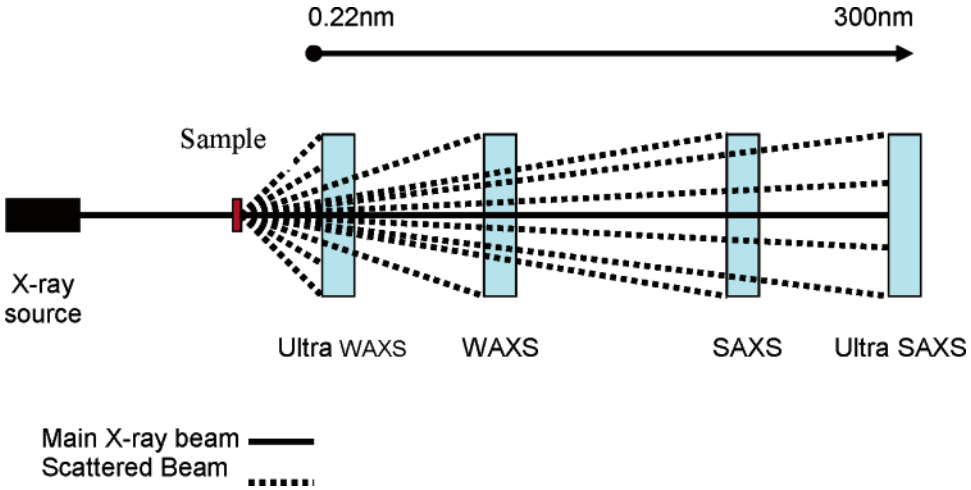

Figure 2. Illustration of sample to detector distances covering UWAXS to USAXS scattering angles. The range of structural features that can be obtained is in the region of 0.22 up to 300 nm.

Table 1. List of Bovine Hide Samples ($n = 3$ for Each Process Stage) Supplied by W. Visscher from William Cowley, Parchment and Vellum Works, Newport Pagnell, U.K.[a]

bovine hide wet	bovine hide dry
untreated (control)	untreated
salted	salted
limed	limed
delimed	delimed
n/a	parchment (control)

[a] Hydrated untreated hide was used as a control. Completed parchment is in a dehydrated state and was therefore used only as a control for the dried samples.

Materials And Methods

Treated Skin Samples. The treated animal skins were supplied by W. Visscher from William Cowley, parchment and vellum works, Newport Pagnell, U.K. The samples selected were calfskin which had been treated in a traditional parchment liming manufacturing process. Due to exact methods being subject to proprietary, a detailed description of the manufacturing process will not be disclosed, but typically salting is used for preservation before processing, followed by soaking the skin in slaked lime for up to 2 weeks for dehairing and removal of proteoglycans and other noncollagenous macromolecules. Deliming of skins involves the use of washing in water and the addition of neutralizing salts.[10]

The control samples used were untreated, mechanically dehaired skin (scraped using a blunt knife; the presence of hair keratin was not observed in X-ray diffraction images and therefore discounted as a possible cause of interference) and parchment representing the start and end products of the process. Table 1 contains a list of the samples used including the dry samples, which were obtained by slowly air-drying a portion of the hydrated samples at room temperature over a 7 day period.

X-ray Scattering Technical Details. X-ray scattering images were obtained and used to analyze the effects of selected stages of the parchment manufacturing process on collagen. By using a series of camera lengths (Figure 2) information was obtained regarding the intra- and intermolecular and intra- and interfibrilar interactions.

The NanoSTAR facility at Cardiff University, with a sample to detector distance of 4 cm, gives ultra wide-angle X-ray scattering (UWAXS) patterns allowing features of collagen structures of between 0.22 and 3.0 nm to be observed. A 0.154 nm X-ray beam is generated by a Kristalloflex 760 X-ray generator (Bruker AXS, Germany) and focused using cross-coupled Göbel mirrors and a 3-pinhole collimation system. A HI−STAR 2d detector is used for data collection. The NanoSTAR was used to measure the changes in the axial rise per residue distance of the collagen helix and the contributions of collagen and amorphous matter to the X-ray diffraction image. Calibration standard was calcite.

Wide and small-angle X-ray scattering (WAXS and SAXS) data were obtained from experiments carried out at SRS Daresbury, U.K., beam line station 2.1, which has a fixed X-ray wavelength of 0.154 nm and a variable sample to camera (multiwire detector) length of 0.9 to 8.0 m giving information on structures in the range from 1 to 200 nm. The sample holder has a computer controlled X−Y elevation stage for movement of the sample in specific and measurable directions.[11] A 1.25 m sample to detector distance was used to obtain WAXS data to evaluate accurately the intermolecular lateral packing of the collagen molecules, which occurs in real space, in the region of ~1 nm in the dehydrated state. The sample to detector distance was increased to 8 m to allow SAXS experiments to observe long-range interactions of

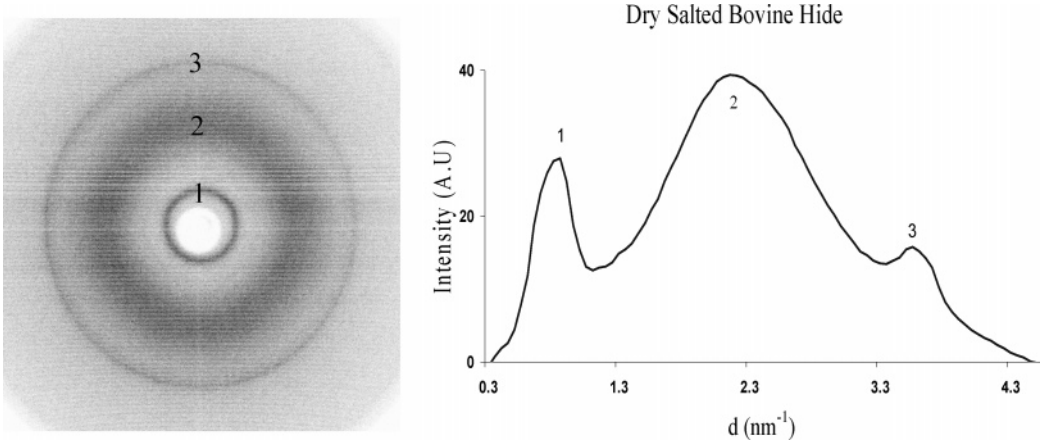

Figure 3. (Left) Wide-angle X-ray diffraction pattern obtained on the NanoSTAR at Cardiff University of salted bovine hide at a sample to detector distance of 4 cm, allowing dimensions in the region of 10−0.2 nm to be resolved. (Right) Linear intensity profile of the 2D image. Peak 1 is representative of the scatter related to the intermolecular lateral packing of the collagen molecules. Peak 2 contains the amorphous scatter. Peak 3 corresponds to the periodicity of the axial rise per residue.

collagen resulting from axial order (*d* spacing). Calibration standards used were silver behenate at 1.25 m and hydrated rat tail tendon at 8 m sample to detector distance.

Ultra small-angle X-ray scattering (USAXS) experiments were carried out on station ID02 at the European Synchrotron Radiation Facility (ESRF, Grenoble, France). This station utilizes a highly collimated, monochromatic intense beam in a pinhole configuration on to a XRII−FReLoN CCD area detector. At a wavelength of 0.1 nm and a sample to detector distance of 10 m, structural information up to 300 nm is obtained from a beam size and detector resolution of 100 μm.[12] Hydrated rat tail tendon was used as a calibration standard. The ultra small-angle X-ray scattering patterns of bovine hide obtained at station ID02 gave a sufficient resolution to determine scattering features due to the cylindrical nature of collagen fibrils and the interference between fibril structures.

The 2-D diffraction patterns were converted into 1-D linear intensity profiles using CCP13 software without significant loss of data.[13] PeakFit4 (AISL software) the one-dimensional peak fitting program was used to determine the peak size shapes and integrated intensity of the linear profiles.

Collagen in both skin and parchment is arranged in a felt-like network; the isotropy of the felt-like arrangement of the collagen fibers[14] within animal hide samples usually results in a radially averaged diffraction image. Preferential alignment of collagen in skin is occasionally seen, but this is most likely due to the location that the sample was taken from, such as collagen fibers taken from the neck and spinal areas.[6]

Results

Evaluation of the Diffraction Data. X-ray scattering patterns of collagen obtained by UWAXS display diffraction series corresponding to axial repeating structures. The position of the strong reflection at approximately 0.29 nm[15] relates to the axial rise distance (helical rise per residue) between the amino acid residues along collagen molecular triple helices. The typical isotropy of a wide angle diffraction pattern from bovine hide and its linear trace of intensity versus scattering angle are shown in Figure 3.

Further analyses using Peakfit4 software of the linear profiles are given in Table 2. The helical rise per residue value of the collagen molecules appears to be relatively unchanged following different treatments. The full width half-maximum of the axial rise per residue peak in Figure 3 increases from untreated skin through to parchment where the greatest change is observed due to the liming of bovine hide.

Table 2. Axial Rise per Residue and Peak Full Width Half Maxima (fwhm) Measurements of Treated Bovine Hide, and the Collagen to Amorphous Ratio

bovine hide	axial rise per residue (nm)	full width half maxima (nm^{-1})	collagen/ amorphous ratio
untreated	0.278	3.23	0.14
salted	0.277	3.95	0.17
limed	0.279	4.89	0.18
delimed	0.279	4.08	0.17
parchment	0.29	5.96	0.18

Collagen/Amorphous Ratio. Gelatinization is caused by a loss of structural order within collagen due to unfolding of the molecules forming gelatin.[16] Dividing the integrated intensity of the peak that accounts for the intermolecular lateral packing of the collagen molecules by the peak arising from the amorphous scatter that result from gelatin and other noncollagenous materials, it is possible to determine a ratio of collagen to amorphous content within the samples.[16,17] Table 2 shows that the ratio of collagen to amorphous material increases as the untreated skin is treated with sodium chloride and then calcium hydroxide.

Changes in Intermolecular Lateral Packing. An X-ray diffraction image displaying the collagen molecule−molecule interactions (intermolecular lateral packing) observable at 1.2 nm[7] is shown in Figure 4. The X-ray diffraction patterns obtained were plotted as linear traces of intensity versus scattering angle, which were analyzed using Peakfit4 software, and the structural information obtained is shown in Table 3.

Salting of bovine hide induces an increase from 1.4 to ∼1.5 nm in the intermolecular lateral packing distance between the collagen molecules in the hydrated state compared to untreated skin. The full width half-maximum of the intermolecular lateral packing reflection of the diffraction pattern in Figure 4 is reduced slightly by salting. These results show that salting induces a greater average distance between collagen molecules but has a minimal effect on the collagen crystallinity.

Liming of the bovine hide increases the distance between the collagen molecules by ∼0.15 nm compared to untreated skin. The full width half-maximum of the peak at ∼1.55 nm is reduced after liming.

Deliming of the sample does not appear to have an effect on the intermolecular lateral packing distance indicating that the

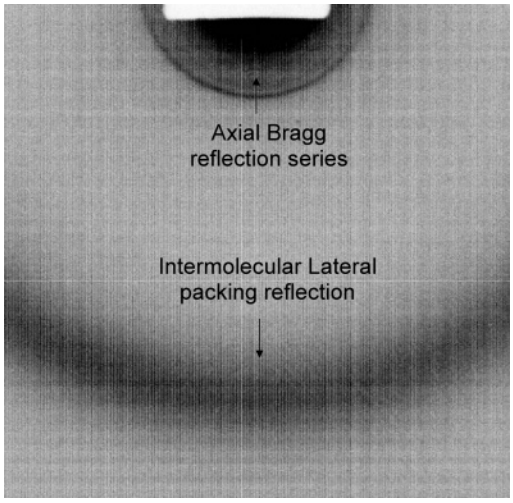

Figure 4. X-ray diffraction pattern obtained at SRS Daresbury station 2.1 of limed bovine hide at a sample to detector distance of 1.25 m, allowing dimensions in the region of 1 nm to be resolved.

liming stage has induced a permanent change in the collagen hierarchical stability. Table 3 shows that after dehydration the collagen molecule-to-molecule distance reduces to ~1.2 nm for all samples and that there is little variation in the full width half-maxima of the intermolecular lateral packing peak.

***d* Spacing.** Collagen exhibits a number of long-range interactions resulting from axial order and possible substructures within the fibril. To observe large-scale features by X-ray diffraction, small angle scattering is used.

The electron density profile of the *d* spacing produces a diffraction series of sharp reflections on the small angle scattering image as shown in Figure 5, panels a and b.[14] These sharp reflections can be used to determine a change in the *d* spacing of the collagen molecules as the alteration in electron density along the fiber axis are reflected in changes to the intensity of these peaks. A useful indicator of sample hydration can be obtained from the reflection intensities, where a strong 5th order of diffraction indicates high levels of hydration and a strong 6th order of diffraction indicates dehydration[3] as shown in Figure 5. Changes to the *d* spacing have been listed in Table 4 for all sample treatments and also the effect of dehydration. Both salting and drying of bovine hide do not appear to have an effect on the collagen *d* spacing. However, liming of bovine hide causes a reduction by ~1 nm giving a value that is similar to the 63.5 nm of parchment.

Fibril Diameter and Packing. The scattering from a fibril is conveniently represented by the scattering of a solid cylinder with a given diameter. The scattering function of such a cylinder is conveniently described as a first-order Bessel function (for example Eikenberry et al., 1982).[18] The ultra small-angle X-ray scattering (USAXS) pattern of bovine hide (Figure 6) obtained at station ID02 of the ESRF gave a sufficient resolution to

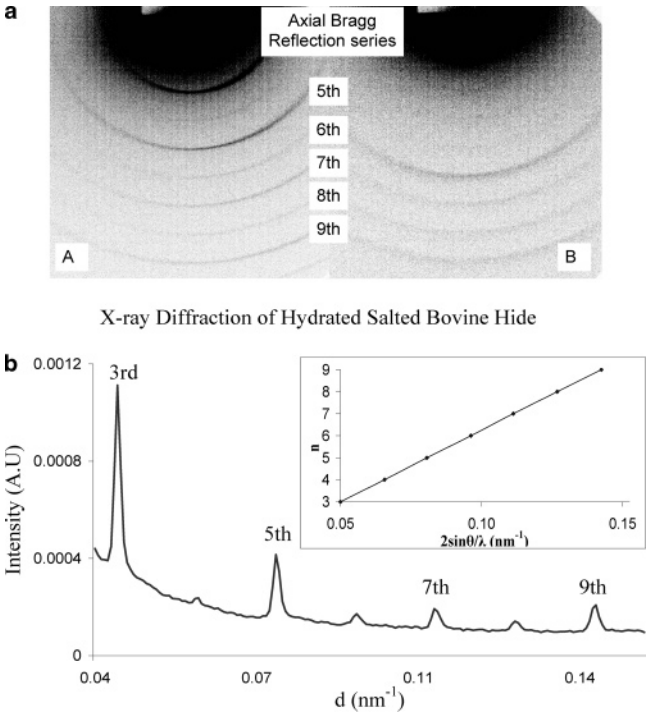

Figure 5. (a) X-ray diffraction pattern obtained at SRS Daresbury station 2.1 of bovine hide at a sample to detector distance of 8 m, allowing dimensions in the region of 200 nm to be resolved. (A) Wet salted hide. (B) Dry salted hide. (b) A linear intensity profile of the small angle diffraction image of hydrated salted bovine hide represented in Figure 5. The orders of Bragg reflections due to the electron density distribution of the gap and overlap interactions of collagen molecules in the axial direction have been included. The positions of these orders with respect to each other, and calibration against a known standard were used to calculate the *d* spacing of the axial gap and overlap. Insert plot is an example of n orders vs 2 sin θ/λ, where the slope is equal to the *d* spacing.

determine scattering features due to the convolution of the Bessel function from the cylindrical nature of the collagen fibrils and the interference function due to the interactions between neighboring fibrils.[8,9]

A linear intensity profile of a Bessel function has maxima at $qr = 0.0$, 5.14. 8.42, 11.6, 14.8, where $q = (4\pi/\lambda) \sin \theta$ (λ = X-ray wavelength and θ = half of the scattering angle) and r is the cylinder radius.[15] Plotting the normalized intensity from a cylindrical object against q, the collagen fibril radii were obtained from the position of these maxima in reciprocal space as shown in Table 5.

The interference function is dependent on the relative positions of the cylinders (fibrils), and a linear intensity profile against the scattering vector q can be used to determine the nearest neighbor center-to-center spacing.[18] Table 5 shows that after liming the fibril diameter increases by ~11 nm and that

Table 3. Collagen Intermolecular Lateral Packing and Peak Full Width Half Maxima (fwhm) Measurements of Bovine Hide in Its Wet and Dry States

bovine hide (wet)	intermolecular lateral packing (nm) (± 0.012 nm)	full width half maxima (nm^{-1})	bovine hide (dry)	intermolecular lateral packing (nm) (± 0.251 nm)	full width half maxima (nm^{-1})
untreated	1.40	1.83	untreated	1.20	1.01
salted	1.49	1.70	salted	1.20	1.05
limed	1.55	1.57	limed	1.17	1.01
delimed	1.57	1.61	delimed	1.18	1.02
			parchment	1.16	1.04

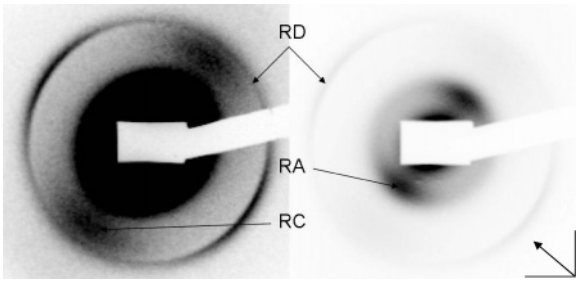

Figure 6. Diffraction pattern of limed bovine skin obtained at ESRF station ID02. The left and right images are used to illustrate how adjusting the minimum and maximum intensity limits of the same image can highlight the features present within the diffraction pattern. The sample to detector distance was 10 m, which was sufficient to observe; (RA) the interference due to the interaction between fibril cylinders, (RC) the 5.14 maxima of the fibril cylinder Bessel function. (RD) The 1st order Bragg reflection due to the electron density distribution of the gap and overlap interactions of collagen molecules in the axial direction. Orientation of the long fiber axis is indicated by the arrow on the bottom right of figure.

Table 4. *d* Spacing of Bovine Hide in Its Wet and Dry States

bovine hide (wet)	d spacing (nm) (± 0.283 nm)	bovine hide (dry)	d spacing (nm) (± 0.141 nm)
untreated	65.3	untreated	65.3
salted	65.0	salted	64.9
limed	64.2	limed (np1)	64.1
delimed	64.1	delimed	not visible
parchment	n/a	parchment	63.5

Table 5. Values for Fibril Lateral Packing, Peak Full Width Half Maxima Measurements and Fibril Diameters of Bovine Hide

bovine hide wet samples	fibril diameter (nm) (± 2.33 nm)	fibril lateral packing (nm) (± 1.13 nm)	full width half maxima (nm^{-1})
untreated	103.2	122.6	0.013
salted	not visible	not visible	not visible
limed	114.5	134.8	0.012
delimed	115.6	136.1	0.013

deliming of the sample does not appear to have an effect on the packing at the suprafibriller level.

The mean center-to-center distance from Table 5 shows that liming of the bovine hide increases the distance between the fibrils. The full width half-maxima of the interference function from Figure 7 does not change, indicating that there is no change in the level of disorder or crystal size. Deliming seems not to have any effect on the collagen fibril packing.

Discussion

The effects of processing hides on the structure of collagen, from the molecular to the fibrillar structures, have been evaluated by X-ray diffraction.

UWAXS described the effects of treatments at the molecular level. Results show that salting and liming do not have an effect on the distance between residues in the axial direction. However, the increased peak width due to liming gave a clear indication of changes at the molecular level. This broadening may be a result of an increase in disorder, a reduction in crystallite size, or a combination of the two. These effects could be due to the high alkalinity of the lime liquor which has been shown to cause a partial hydrolysis of the polypeptide backbone and to hydrolyze the amide groups.[19] The hydrolysis of the polypeptide

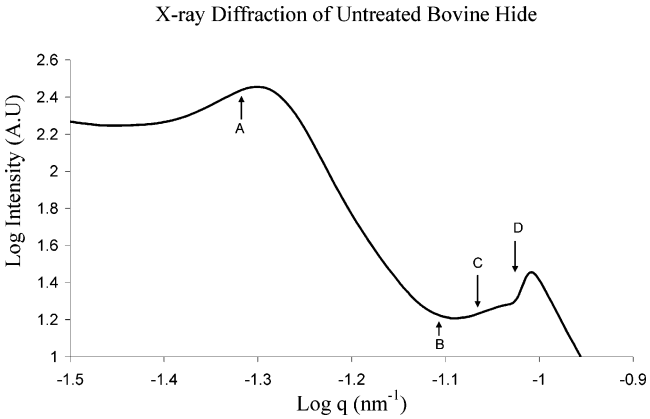

Figure 7. Linear profile of an ultra small angle diffraction image of untreated bovine hide. (A) The interference due to the interaction between fibril cylinders. (B) The 3.83 minima of the fibril cylinder Bessel function. (C) The 5.14 maxima of the fibril cylinder Bessel function. (D) The 1st order Bragg reflection due to the electron density distribution of the gap and overlap interactions of collagen molecules in the axial direction.

chains may be expected to alter the axial rise per residue distance at the point of hydrolysis; alternatively, several breakages in the collagen helix could lead to local relaxation of structure. The change of the amino acids from the L to D forms may have an effect on the distance between neighboring residues. Results indicate that although there is not an overall change in axial rise per residue distance, after salting or liming there is a breakdown in the local crystallinity, which could be explained by local effects such as hydrolysis and racemisation.

WAXS was employed to describe the interactions between neighboring collagen molecules. Salting of bovine hide increases the intermolecular lateral packing between collagen molecules and increases the level of disorder. This indicates that water or salt may be entering the spaces between the collagen molecules within the fibrils and that the fibrils are expanding.

Following liming, the intermolecular lateral packing peak becomes narrower, indicating that there may be a reduction in local disorder. The results demonstrate that this is accompanied by a swelling at the molecular level. The presence of Ca^{2+} ions from the lime is thought to cause an influx of water molecules causing the fibers to swell.[6] The high alkalinity of the lime solution shifts the iso-electric point causing some of the charges along the molecule to change, altering the side chain interactions between the molecules. This combined with hydrolysis of the side chains, which reduces the number of sites available for salt bridge cross linkages, may cause a lowering of stability.[5] Weakening of intermolecular collagen interactions and the influx of water may cause the loosening of the fiber network as found here.

SAXS showed that there was a reduction in *d* spacing after liming, which is most likely due to a change in the fibrillar structure in the axial direction. The weakening of side chain interactions due to hydrolysis and the change in the isoelectric point induced by the high alkalinity of the lime liquor may allow the possibility of the collagen molecules to move past each other, particularly if there was a reduction in intermolecular cross-links. Drying of the samples does not appear to have an effect on the *d* spacing indicating that the contraction is due to liming and not dehydration.

Collagen interactions with proteoglycans are fundamental to fibril diameter and packing. Proteoglycans are involved in dissipating compression stresses in the skin and are also involved in alignment of collagen fibrils.[4] The polysaccharide hyaluron

connects the decorin protein cores associated with dermatan sulfate bridges, which act as a compression resistive bridge between the fibrils. Salting of skin has been shown to remove up to 100% of the hyaluron,[6] but it requires the liming stage to remove over 50% of dermatan sulfate. The removal of hyaluron may release the pressure constraint on the fibrils, allowing the collagen fibrils to expand, and the "opening up" of the collagen fibers.

The results here show that after salting there is an increase in the distance between the collagen molecules in the hydrated state, and even more expansion after liming, which is carried through the hierarchical levels up to fibril packing; deliming did not appear to reverse these increases, indicating that the effects of salting and liming are permanent.

The removal of noncollagenous material due to the lime liquor is responsible for the increase in the collagen/amorphous ratio indicating that there is less amorphous material in comparison to collagen. If the collagen ratio had decreased, this would have indicated that the collagen molecules had become denatured. However, our results imply that the collagen structure and hierarchy although weakened are still relatively stable.

Conclusions

A general statement that the collagen fibers within the animal hide "open up" due to processing stages has been widely accepted. Our X-ray diffraction studies now quantitatively describe a swelling in fiber structure at the molecular level, which is observed through the hierarchical levels of collagen. Altering the amino acid side chains of the collagen molecules is likely to reduce stability between the molecules. This combined with the influx of water and the removal of proteoglycans from between the fibrils is most likely to be the cause of the "opening up" of the collagen fibers. However, the most noticeable structural change due to liming is the reduction in the *d* spacing. This combined with the helical rise per residue distance being unaffected is an indication that most of the changes are due to intermolecular interactions of collagen molecules as opposed to intramolecular.

Acknowledgment. We wish to thank Gunter Grossman, Station Manager of Beamline 2.1, Daresbury, U.K. and Thomas Weiss, Beamline ID02, ESRF, Grenoble, France for technical assistance and advice. We would also like to thank W. Visscher from William Cowley, Parchment and Vellum Works Newport Pagnell, U.K. for kindly supplying samples.

Note Added after ASAP Publication. An additional acknowledgment was added to the paper that was originally published on the Web on July 22, 2006. The corrected version was reposted on August 4, 2006.

References and Notes

(1) De Clercq, M. *J. Imaging Sci. Technol.* **1995**, *39*, 367−372.
(2) Obrink, B. *Eur. J. Biochem*. **1973**, *33*, 387−400.
(3) Stinson, R. H.; Sweeney, P. R. *Biochim. Biophys. Acta* **1980**, *621*, 158−161.
(4) Scott, J. E. *Pathol. Biol.* **2001**, 49, 284−289.
(5) Cameron, G. J.; Alberts, I. L.; Laing, J. H.; Wess, T. J. *J. Struct. Biol*. **2002**, *137*, 15−22.
(6) Haines, B. M. *Parchment, The physical and chemical characteristics of parchment and the materials used in its conservation*; The Leather Conservation Centre: Northampton, 1999.
(7) Sionkowska, A.; Wisniewski, M.; Skopinska, J.; Kennedy, C. J.; Wess, T. J. *Biomaterials* **2004**, *25*, 795−801.
(8) Goh, K. L.; Hiller, J. L.; Haston, D. F.; Holmes, K. E.; Kadler, A.; Murdoch, Meakin, J. R.; Wess, T. J. *Biochim. Biophys. Acta* **2005**, *1722*, 183−188.
(9) Quantock, A. J.; Meek, K. M.; Chakravarti, S. *Invest. Ophthalmol. Vision Sci*. **2001**, *42*, 1750−1756.
(10) Kolomaznik, K.; Blaha, A.; Dedrle, T.; Bailey, D. G.; Taylor, M. M. *J. Am. Leather Chem. Assoc.* **1996**, *91*, 18−20.
(11) Grossmann, J. G. In *Scattering*; Pike, P. S. E. R., Ed.; Academic Press: London, 2002; pp 1123−1139.
(12) Narayanan, T.; Diat, O.; Bosecke, P. *Nucl. Instrum. Methods A* **2001**, *467−468*, 1005−1009.
(13) Wess, T. J.; Drakopoulos, M.; Snigirev, A.; Wouters, J.; Paris, O.; Fratzl, P.; Collins, M.; Hiller, J.; Nielsen, K. *Archaeometry* **2001**, *43*, 117−129.
(14) Wess, T. J.; Orgel, J. P. *Thermochim. Acta* **2000**, *365*, 119−128.
(15) Meek, K. M.; Quantock, A. J. *Prog. Retin. Eye Res*. **2001**, *20*, 95−137.
(16) Weiner, S.; Kustanovich, Z.; Gil-Av, E.; Traub, W. *Nature* **1980**, *287*, 820−823.
(17) Kennedy, C. J.; Hiller, J.; Lammie, D.; Drakopoulos, M.; Vest, M.; Cooper, M.; Adderley, W. P.; Wess, T. J. *Nano Lett.* **2004**, *4*, 1373−1380.
(18) Eikenberry, E. F.; Brodsky, B.; Parry D. A. D. *Int. J. Biol. Macromol*. **1982**, *4*, 322−328.
(19) Menderes, O.; Covington, A. D.; Waite, E. R.; Collins, M. J. *J. Soc. Leather Tech. Chem.* **1998**, *83*, 107−110.

BM060250T